frontiers | Frontiers in Marine Science

TYPE Original Research
PUBLISHED 24 November 2023
DOI 10.3389/fmars.2023.1301449

OPEN ACCESS

EDITED BY
Luca Parma,
University of Bologna, Italy

REVIEWED BY
Carlos Alfonso Alvarez-González,
Universidad Juárez Autónoma de Tabasco, Mexico
Luciana Mandrioli,
University of Bologna, Italy

*CORRESPONDENCE
Luis A. Salazar
luis.salazar@ufrontera.cl

RECEIVED 25 September 2023
ACCEPTED 06 November 2023
PUBLISHED 24 November 2023

CITATION
Godoy K, Sandoval C, Vásquez C, Manterola-Barroso C, Toledo B, Calfuleo J, Beltrán C, Bustamante M, Valderrama S, Rojas M and Salazar LA (2023) Osteogenic and microstructural characterization in normal versus deformed jaws of rainbow trout (*Oncorhynchus mykiss*) from freshwater.
Front. Mar. Sci. 10:1301449.
doi: 10.3389/fmars.2023.1301449

Osteogenic and microstructural characterization in normal versus deformed jaws of rainbow trout (*Oncorhynchus mykiss*) from freshwater

Karina Godoy[1,2,3], Cristian Sandoval[4,5], Claudio Vásquez[2,3,6], Carlos Manterola-Barroso[3], Barbara Toledo[3,7], Joel Calfuleo[3,7], Carolina Beltrán[3], Marion Bustamante[8], Sebastián Valderrama[9], Mariana Rojas[1,10] and Luis A. Salazar[2,3,6]*

[1]Programa de Doctorado en Ciencias Morfológicas, Facultad de Medicina, Universidad de La Frontera, Temuco, Chile, [2]Centro de Biología Molecular y Farmacogenética, Departamento de Ciencias Básicas, Facultad de Medicina, Universidad de La Frontera, Temuco, Chile, [3]Núcleo Científico y Tecnológico en Biorecursos (BIOREN), Universidad de La Frontera, Temuco, Chile, [4]Escuela de Tecnología Médica, Facultad de Salud, Universidad Santo Tomás, Osorno, Chile, [5]Departamento de Ciencias Preclínicas, Facultad de Medicina, Universidad de La Frontera, Temuco, Chile, [6]Doctorado en Ciencias, Mención Biología Celular y Molecular Aplicada, Universidad de La Frontera, Temuco, Chile, [7]Carrera de Química y Farmacia, Facultad de Medicina, Universidad de La Frontera, Temuco, Chile, [8]Departamento de Obras Civiles, Facultad de Ingeniería y Ciencias, Universidad de La Frontera, Temuco, Chile, [9]ADL Diagnostic Chile SpA, Villarrica, Chile, [10]Programa de Anatomía y Biología del Desarrollo, Instituto de Ciencias Biomédicas (ICBM), Facultad de Medicina, Universidad de Chile, Santiago, Chile

Introduction: During the processes of formation and maturation of farmed salmonids, bone deformities could be associated with changes in the mineralization levels of the axial skeleton and the bone-signaling pathways. Therefore, we aimed to evaluate the gene expression during bone formation and regeneration and their relationship with mineralization in rainbow trout with mandibular deformation.

Methods: We included five normal fish and five specimens with mandibular deformation in smolt rainbow trout weighing 400 g and measuring 25 to 35 cm in length. We assessed 1. serum metabolites, 2. microstructure and mandibular bone mineralization and, 3. gene expression of bone signaling pathways. These analyses were done to determine the main causes and/or mechanisms of deformity.

Results and discussion: Our results show a marked elevation of bone morphogenetic protein 2 (Bmp2). Also, we found a distinct expression pattern for transcriptional factors, observing diminished RUNX family transcription factor 2 (Runx-2) expression coupled with a simultaneous elevation of osterix (Osx) levels. We also observed decreased osteocalcin and alkaline phosphatase levels related to mineral content loss and an increase in collagen type I as a compensatory structural response. In conclusion, rainbow trout deformation was characterized by demineralization, increased porosity without destruction of the organic matrix, and a moderate decrease in bone mineral content.

KEYWORDS

aquaculture, bone, gene expression, microelements, scanning electron microscopy

1 Introduction

Bone deformation is a multifactorial pathology of fish mainly associated with environmental, nutritional, and genetic factors (Iaria et al., 2021). More importantly, its incidence is considered a quality index (Boglione et al., 2013; Le Luyer et al., 2015; Lall and Kaushik, 2021). Environmental and nutritional factors related to management conditions, physicochemical characteristics, fish density, nutrients, and microelement composition within the diet (Boglione et al., 2013). At the same time, genetic factors such as the aberrant expression of genes participating in processes like bone tissue formation, remodeling, and repair can also affect different and relevant pathways (Krossøy et al., 2009; Boglione et al., 2013).

Many genes have been implicated in different stages of skeleton formation in salmonids, constituting a complex of highly regulated signaling pathways represented by families such as bone morphogenetic proteins (Bmps), waterproof (Wat), and neurogenic locus notch homolog protein (Notch) proteins (Day et al., 2005; Lin and Hankenson, 2011; Zhao et al., 2019). During osteogenesis, the expression of sonic hedgehog (Shh) genes involved in axial bone growth, the spine, and fins (Olivares and Rojas, 2013) and homeobox (Hox) genes related to skull and tooth growth regulate the activation of these signaling pathways (Theslelf, 1995; Liu et al., 2004; Lin and Hankenson, 2011).

BMPs represent one of the best-described pathways, with more than 30 isoforms reported. Bone morphogenetic protein 2 (BMP2), bone morphogenetic protein 4 (BMP4), bone morphogenetic protein 5 (BMP5), bone morphogenetic protein 6 (BMP6), bone morphogenetic protein 7 (BMP7), bone morphogenetic protein 8 (BMP8), bone morphogenetic protein 9 (BMP9), bone morphogenetic protein 11 (BMP11), bone morphogenetic protein 12 (BMP12), bone morphogenetic protein 13 (BMP13), and bone morphogenetic protein 14 (BMP14) have osteogenic activity (Dumic-Cule et al., 2018). However, one of the critical BMP markers corresponds to *Bmp2*/BMP2 since it allows bone regeneration by activating the expression of transcription factors such as SRY-box transcription factor 9 (Sox9), RUNX family transcription factor 2 (Runx2), and Osterix (*Osx*), leading to bone formation and development (Ducy et al., 1997; Kirkham and Cartmell, 2007; Matsubara et al., 2008; Lin and Hankenson, 2011).

Runx-2 has been a transcription factor considered an exclusive marker of mineralized tissues, playing a central role during osteogenesis (Kirkham and Cartmell, 2007). Its activation directly stimulates the transcription of genes such as osteocalcin, osteopontin, collagen I, collagenase 3 (matrix metalloproteinase 1), sialoprotein, and alkaline phosphatase (ALP), all related to extracellular matrix formation (Ducy et al., 1997; Franceschi and Xiao, 2003; Kirkham and Cartmell, 2007; Lin and Hankenson, 2011). Osterix, also known as transcription factor Sp7, is another transcription factor essential for osteoblast differentiation and bone construction (Nakashima et al., 2002; Kirkham and Cartmell, 2007). Its activation has been related to the formation, development, and maturation of bone tissue during embryogenesis, the formation of new bone and osteoblast differentiation (Komori et al., 1997; Nakashima et al., 2002; Kirkham and Cartmell, 2007; Matsubara et al., 2008; Zhou et al., 2010; Sinha and Xin Zhou, 2013).

Among the proteins involved in bone matrix formation, the most relevant are osteocalcin (OCN), collagen type I (COL-I), and alkaline phosphatase (ALP). Osteocalcin is a protein secreted by osteoblasts as part of the extracellular matrix and is the most abundant of the non-collagenous proteins (Koga et al., 2005; Fernández-Tresguerres et al., 2006; Perez-Amodio et al.; 2006; Hayman, 2008). Collagen type I is an extracellular matrix protein in bone tissue and represents the most important and abundant of the collagen proteins found in bone (Matsubara et al., 2008; Gistelinck et al., 2016). The expression of Col-I has been considered an early marker of osteoblast activity and plays a crucial role in osteoblast differentiation (Matsubara et al., 2008). According to research, rainbow trout have a subunit composition of 1 (I), 2 (I), and 3 (I), with 3 (I) being specific for bone (Saito et al., 1998; Saito et al., 2001).

Alkaline phosphatase, due to its wide distribution in the body and the many isoenzymes it presents in the blood, saliva, liver, and kidney, represents an excellent early clinical marker for multiple pathologies in fish (Congleton and Wagner, 2006; Matsubara et al., 2008). Osteoblasts produce the bone ALP fraction, a feature of phenotypic differentiation, proliferation, and migration (Matsubara et al., 2008). Plasma levels of ALP represent a marker of osteoblastic activity (Delmas et al., 2000; Kuo and Chen, 2017). Moreover, there was a direct relationship between the presence of ALP and the correct mineralization of bone tissue in vertebrates (Delmas et al., 2000; Fernández-Tresguerres et al., 2006; Kuo and Chen, 2017). Another phosphatase fraction in bone tissue is an acid phosphatase, a marker of tartrate-resistant acid phosphatase (TRAP) activity (Fernández-Tresguerres et al., 2006; Perez-Amodio et al., 2006; Hayman, 2008). Finally, calcium and phosphorus in both bone and plasma represent systemic regulation of bone formation and remodeling, as these minerals are bioavailability indicators (Beck et al., 2000; Sugiura et al., 2003; Pombinho et al., 2004). Therefore, we aimed to evaluate the changes in the expression of genes involved in formation and regeneration and their relationship with bone mineralization in rainbow trout with mandibular deformation.

2 Materials and methods

2.1 Sampling and bone tissue collection

In the salmon farming industry in Chile, three different species of salmonids are farmed, mainly *Salmo salar*, followed by Salmon coho (*Oncorhynchus kisutch*) and, to a lesser extent, rainbow trout. The production model is subdivided into two parts: fresh water and sea. Currently, fresh water is delivered through open flow centers (rivers, springs, wells), as well as in recirculation systems; however, in the sea, it is only done through a culture cage module in a completely open flow system. The cultivation of the specimens is under strict inspection control for SERNAPESCA aquaculture, with different standards and active surveillance programs: Exempt Resolution N° 1.577/2011

(Ministerio de Economía, Fomento y Turismo et al., 2023b), Exempt Resolution N° 228/2013 (Ministerio de Economía, Fomento y Turismo et al., 2023a) and Exempt Resolution N° 3610/2019 (Ministerio de Economía, Fomento y Turismo et al., 2023c).

We selected and collected specimens of juvenile (smolt) freshwater rainbow trout of 25 to 35 cm in size, weigh <400 g, from pre-cordillera fish farming in the La Araucanía region (Chile). The fish were farmed under general standards (water temperature of 12°C, dissolved oxygen of 8.5 ppm, carbon dioxide <7 ppm, pH 6.5 to 8.5, and antibiotic concentration of 0.002–6.0 µg/L). The capture of farmed fish was realized by authorized fish farming personnel. The ten specimens were then divided into two groups: five clinically normal control specimens with no deformation (Group 1), and five specimens with jaw deformities (Group 2).

Both groups were anesthetized to obtain blood samples with benzocaine 20% (Veterquimica S.A., Chile) at 30–40 ppm. Subsequently, they were euthanized by overexposure to the anesthetic for more than 10 minutes. Blood samples and specimens were stored at 0°C in a container with ice during 4 h (Supplementary Figure 1). The Scientific Ethics Committee of the Universidad de La Frontera has approved the experimental protocol (N°061_20).

2.2 Sample processing

Blood samples were centrifuged at 1500 rpm, and the serum was separated from the cellular component and stored at -20°C until further analysis. The euthanized specimens were decapitated. Blood samples were obtained and immediately frozen in cryotubes at -80°C until analysis. For microstructure analysis, the samples were dissected to remove the skin, muscle, connective tissue, and other organic components by treating them with deionized water at 60–70°C for about 20 min to facilitate the removal of tissue, leaving the inorganic component to interfere free without altering the structure. Then, were fixed with glutaraldehyde 1.5% in 0.1 mol of cacodylate buffer pH 7.4. The samples were analyzed by Scanning Electron Microscopy - Energy Dispersive X-ray spectroscopy detector (SEM-EDX) and subsequently reduced to a fine powder by pulverization with a thermogravimetric analysis and differential scanning calorimetry (TGA-DSC) and porosity analyses. For gene expression, the jaw was dissected to remove the skin, muscle, connective tissue, and other organic components, which were immediately frozen in cryotubes at -80°C until analysis.

2.3 Quantification of serum metabolites

Serum samples were thawed at room temperature. Total proteins, albumin, globulins, glucose, phosphatase activity, and microelements (calcium, phosphorus, iron, and magnesium) were quantified in a multimodal Synergy HT reader (BIOTEK, Winooski, VT, USA) following the manufacturer's protocol (Human Diagnostics, Wiesbaden, Germany).

2.4 Microstructure and mandibular bone mineralization

2.4.1 Microstructure and microelemental analysis by scanning electron microscopy coupled with EDX

The fixed mandibular bone samples were washed with distilled and deionized water three times and dried in an oven at 25°C for 24 hours. The dried sample was adhered to the sample holder with double-sided carbon tape. The quantification element was coupled to the X-ray energy dispersive spectroscopy detector (EDX), and three quantification points were chosen for each region of interest (ROI), as has been described previously by Godoy et al. (2022). The acquisition was performed under the following parameters: an applied energy of 15 KV, a pressure of 20 Pa, and a WD of 10 mm, using a scanning electron microscope (HITACHI SU3500, Tokyo-Japan) coupled to an XFlash ® Detector 410 and a Quantax ESPRIT 1.8.1 software controller (Bruker, Germany).

2.4.2 Superficial area and porosity analysis in mandibular bone

The powder samples were dried in an oven at 40°C for 48 hours. Approximately 100 mg of the samples (pooled samples) were degasified for 16 hours at 160°C and subjected to a surface area and pore size gas sorption analyzer in mandibular bone (NovaWin-Quantachrome, Boynton Beach, Florida, USA). Data acquisition was realized using NOVA instruments (version 11.03, Florida, USA).

2.4.3 Thermogravimetric analysis and differential scanning calorimetry in mandibular bone

Approximately 20 mg of samples (bone powder, pooled samples) were subjected to two thermogravimetric analyses: first, from 25°C to 850°C (10°C per minute rate) to evaluate bone sample stability in the air atmosphere by monitoring weight loss, and second, differential thermal behavior (DSC) from 25°C to 850°C (50°C per minute rate) (Thermogravimetric Analysis TGA/DSC STA 6000, Perkin Elmer, Waltham, MA, USA).

2.4.4 Crystallographic analysis by X- Ray diffraction in mandibular bone

Approximately 500 mg of bone powder samples (pooled samples) were subjected to analysis. In a diffractometer equipped with a monochromatic copper anode radiation detector SSD160 1D (CuKα, λ = 1.5406 Å), the phases of HPA in mandibular bone were investigated. The diffractograms were obtained in a 20-degree range (5° and 80°), with a step size of 0.061° (total steps of 1236) and a total step time of 0.5 s over a 60-minute period. The sample was analyzed with a diffractometer (2D PHAZER, Bruker, Munich, Germany). Data acquisition was realized using DIFFRAC.SUITE software (Bruker, Munich, Germany).

2.4.5 Functional groups by infrared spectroscopy (FT-IR) in mandibular bone

Approximately 5 mg of bone powder (pooled samples) was mixed with 50 mg potassium bromide powder (KBr-Merck), finely ground manually with an agate mortar, and pressed into 13 mm discs with a manual press. Disc samples (20 mg) were inserted into the system sample chamber for analysis. The characterization of functional groups was analyzed in the mid-infrared from 4000 to 400 cm^{-1} with an FT-IR spectrometer (TENSOR 27, Bruker, Munich, Germany) equipped with a DLATG detector. Data collection and analysis were realized using spectroscopy software (OPUSTM, Bruker, Munich, Germany).

2.5 Bone gene expression

2.5.1 RNA extraction and purification

The samples were ground with liquid nitrogen. Total RNA was extracted using TRIzol™ Plus RNA Purification Kit according to the manufacturer's instructions (ThermoFisher Scientific, USA), and homogenized with zirconium beads in a FastPrep-24™ tube (MP Biomedicals, USA) at 6.5 m/s for 1 minute. DNase treatment eliminated genomic DNA from the samples (ThermoFisher Scientific, USA). The RNA sample extract was transferred and purified on a column according to the manufacturer's instructions (PureLink™ Kit, ThermoFisher Scientific, USA). The fluorimeter (Quit 4 Fluorimeter, ThermoFisher Scientific, USA) was used to assess RNA quality (Supplementary Table 1), and the Multimode Reader (Synergy H1 Hybrid Reader, Take3, Biotek, USA) was used to assess RNA integrity. The RNA was then stored at -80°C before further processing.

2.5.2 Synthesis of cDNA

Purified RNA was incubated with the RT-reaction mix (10 mM dNTPs, 50 ng/µL random hexameters, DECP-treated water) to a 10-µL final volume reaction and set at 65°C for 5 minutes, then cooled quickly on the ice. Subsequently, 2 µL of total RNA were incubated for cDNA synthesis with 9 µL of reaction mix (10X RT buffer, 25 nM $MgCl_2$, 0.1 DTT, and RNase Out 40 U/µL), mixed, and incubated at room temperature for 2 minutes, and then one µL of the mixture was added to each sample (SuperScript II Reverse Transcriptase™, ThermoFisher Scientific, USA). cDNA synthesis was performed in 40 cycles under the following conditions: 10 minutes at room temperature, followed by 50 minutes at 42°C. The reaction was finished at 70°C for 15 minutes, quickly cooled on ice, and 1 µL of RNase H was added to each tube (ThermoFisher Scientific, USA) for incubation at 37°C for 20 minutes (StepONe Plus, Applied Biosystems, Waltham, Massachusetts, USA). The obtained cDNA was stored at -20°C until qPCR analysis.

2.5.3 Fragment amplification by qPCR

The PCR reactions were run in triplicate on strips with the StepOne Plus equipment (Applied Biosystems, Waltham, Massachusetts, USA) using Evagreen 5X Hot Firepol qPCR according to the protocols (Solis BioDyne, Tartu, Estonia). qPCR was achieved with a 12-minute denaturation phase at 95°C, followed by 40 cycles of 15 s at 95°C and 60 s at 60°C. A melting curve analysis of each qPCR was carried out after each cycle. The following genes were evaluated: 1) transcription factors *Runx2* and *Osx*), 2) osteogenic factors *Bmp2* and *Bmp4*, and 3) bone matrix genes *Alp*, *Col-I* and *Ocn* (Table 1, Designed by Larama SPA Informatics, Chile, Syntethized by Macrogen, Seoul, Republic of Korea). The data were normalized according to the mRNA expression levels of housekeeping genes, such as *Ef1a* (Table 1). The number of times the reporter dye in the PCR reaction crossed a software-defined threshold, which was computed automatically by the StepOnePlus™ Software, is referred to as the 'Ct', or threshold cycle (version 2.3, Applied Biosystems, Waltham, MA, USA). The relative expression level of each RNA was estimated using the comparative threshold cycle (Ct) technique ($2^{-\Delta\Delta Ct}$ method) by averaging the Ct values from three replicates. We utilized the threshold cycle values automatically generated by the qPCR equipment for the $2^{-\Delta\Delta Ct}$ technique. The $2^{-\Delta\Delta Ct}$ comparative approach was used to estimate relative gene expression, as has been previously described (Sandoval et al., 2022).

2.6 Statistical analysis

Data normality was analyzed using the D'Agostino-Pearson test for descriptive statistics. The differences between groups were analyzed with the Mann-Whitney U test. The value of $p < 0.05$

TABLE 1 Primers for RT-qPCR.

Gene	Accession number	Forward primer	Reverse primer	Amplicon-Length
Runx2	XM_021613996.1	AAGTTGTGGCATTGGGAGAG	TGCTACTTGAGGAGGGTTGG	212 bp
Ostx	XM_021570138.1	CAGAGGAGGAGGAGAGAGCA	GACATGGAGGTCTGGAAGGA	153 bp
Bmp2	XM_021612508.1	CTGCACAGGGACAAGAGACA	GTTGGTGGAGTTGAGGTGGT	207 bp
Bmp4	XM_021585091.1	ACTCTACCAACCACGCCATC	CACCCTTCCACAACCATTTC	106 bp
Alp3	XM_021587006.1	ATGGGCATTACCACCATCAC	GACCGTGTTCAGGTTGGTCT	201 bp
Col-1	NM_001124177.1	TGCTAATGGAGCCAAAGGAG	TCCATCAGAACCAGGGAAAC	190 bp
Ocn	XM_021567820.1	CCGCATACTATGGACCACCT	ACTTGTGGCTGGTCTTGCTC	205 bp
Ef1a	XM_021580472.1	CCACTGGCCACCTGATCTAC	CCTGCTGGTCTCAAACTTCC	185 bp

was considered statistically significant (GraphPad Software, version 9.0, San Diego, CA, USA).

3 Results

3.1 Blood metabolites and microelements

The values of metabolites and microelements for controls were within the parameters previously observed. Protein, albumin, and globulin content decreased significantly in deformed fish compared with controls. However, phosphatase activity increased in both deformed and normal fish, especially the value of alkaline phosphatase (Table 2).

Although, calcium and magnesium (Mg) seem to show similar levels, significant differences were found between groups ($p<0.001$). In addition, increased phosphorus ($p<0.001$) and decreased iron ($p<0.001$) levels in control and deformed fish were found, respectively (Table 3).

3.2 Microstructure and mandibular bone mineralization

In the micro-structural analysis of a normal fish's mandibular bone, regular bone porosity characteristics were observed (Figure 1A). However, the mandibular bone of deformed fish presents many microstructure defects, including increased fractures, porosity, and hypermineralization zones (Figures 1B–D).

The elemental analysis differed in the percentage of elements. We found higher carbon (C), oxygen (O), calcium (Ca) and phosphorous (P) mass percent (%) values in mandibular bones from normal fish (Figure 2A) in comparison to deformed fish (Figure 2B), but significant differences were found only in the oxygen mass percent ($p = 0.010$).

In the elemental distribution (mapping), we observed roughness, porosity, and micro-fractures present in the microstructure, which coincide with decreased Ca (red) and P (green), as well as increased C (blue), of the bone-deformed mandible (Figure 3B) in comparison to normal fish (Figure 3A).

The elemental analysis of the mandibular bone samples in three ROI zones revealed significant differences in all but one of the elements that were looked at (Table 4). In fact, higher levels of Ca and P in healthy fish were found ($p > 0.05$) as they represent the inorganic component called hydroxyapatite (HPA). Also, higher levels of Mg and fluoride were found because they are necessary for bone metabolism ($p > 0.05$). However, the Ca/P ratio did not differ significantly between the groups. In relation to C, it was higher in deformed fish due to decreased bone mineralization in this group.

3.3 Superficial area and porosity analysis in mandibular bone

Micrographs of the deformed mandibular bone show that it has more pores, but a quantitative analysis showed that the surface area was smaller, which means that the pores are bigger (Table 5).

3.4 Thermogravimetric analysis in mandibular bone (TGA-DSC)

The proximal thermogravimetric analysis showed the loss of mass (blue) due to temperature (red) in the presence of oxygen or oxidative decomposition (Figures 4–7). Both groups recorded mass changes during the combustion time, the first at 2–6 minutes following the loss of water (H°), at 6–14 min, and the last between 18–22 minutes. Humidity, fixed carbon, and volatile compounds derived from carbon and ashes (minerals) values in the mandibular bones of normal fish (Figure 4) and deformed fish (Figure 5) are shown.

Differential scanning calorimetry, or DSC analysis, describes changes in the sample associated with increasing temperature in the absence of oxygen (Figures 6, 7). These mass reductions or transitions occurred at 93.1 °C, 340.6 °C, and 490.6 °C for normal fish (Figure 6), while they occurred at 88 °C, 325.2 °C, and 441.9 °C in deformed fish (Figure 7), with no significant differences in temperature at the transitions between the groups.

3.5 Crystallographic analysis by X-Ray diffraction in mandibular bone

X-ray powder diffraction is an exceptionally potent technique for the qualitative examination of various forms of crystalline solids.

TABLE 2 Blood metabolites in rainbow trout from farmed.

Metabolites	Median (minimum – maximum)		p value
	Normal Fish	Deformed Fish	
Albumin (g/L)	31.85 (20.30 – 40.20)	31.00 (17.51 – 66.20)	0.019
Glucose (mmol/L)	4.29 (1.77 – 5.18)	5.17 (4.18 – 6.33)	<0.001
Globulins (g/L)	25.23 (6.63 – 37.72)	12.69 (1.35 – 23.83)	<0.001
Total Proteins (g/L)	53.26 (44.56 – 74.82)	41.83 (30.05 – 56.58)	<0.001
Acid Phosphatase (U/L)	34.70 (34.50 – 35.20)	39.75 (39.60 – 40.00)	0.029
Alkaline Phosphatase (U/L)	216.55 (193.50 – 257.70)	410.20 (224.70 – 493.00)	0.002

TABLE 3 Blood microelements in rainbow trout from farmed.

Metabolites	Median (minimum – maximum)		p value
	Normal Fish	Deformed Fish	
Calcium (mmol/L)	9.74 (6.88 – 11.00)	9.14 (5.70 – 11.67)	<0.001
Phosphorous (mmol/L)	7.57 (5.64 – 9.70)	10.44 (6.35 – 11.35)	<0.001
Ca/P ratio	1.27 (1.13 – 1.49)	0.87 (0.78 – 0.96)	<0.001
Magnesium (mmol/L)	2.45 (1.47 – 3.17)	2.16 (1.55 – 2.73)	<0.001
Iron (mmol/L)	16.04 (8.37 – 39.75)	6.58 (2.32 – 14.64)	<0.001

All crystalline components of a sample contribute to the total diffraction pattern and can be identified by utilizing data from extensive databases, including commercially available ones (Downs and Hall-Wallace, 2003), open-access databases (Gražulis et al., 2009; Gražulis et al., 2012; Gražulis et al., 2015), and user-created databases. Data obtained from XRD diffractograms showed the main peak of greater intensity corresponding to HPA as hydroxyapatite (H) and fluorapatite (F) at 2θ = 32.5 in both groups (Figure 8). A secondary peak of lesser intensity was also observed at 2θ = 25, which was identified as tri-calcium phosphate (TCP). A small peak corresponding to apatite (A) was also identified in the mandibular bone of normal fish.

3.6 Functional groups analysis by infrared spectroscopy (FT-IR) in mandibular bone

FTIR spectroscopy is a reliable technique used to analyze the structural characteristics of biomaterials (Paschalis et al., 2011; Kowalczuk and Pitucha, 2019). The chemical composition of structures can be assessed and correlated with treatments and pathologies by analyzing the spectrum profile and specific band area ratios (Verdelis et al., 2007; Lubarsky et al., 2012; Liu et al., 2014; Orilisi et al., 2021). The characterization of functional groups for the mandibular bone samples using FT-IR showed similar spectra corresponding to the spectrum of commercial HPA

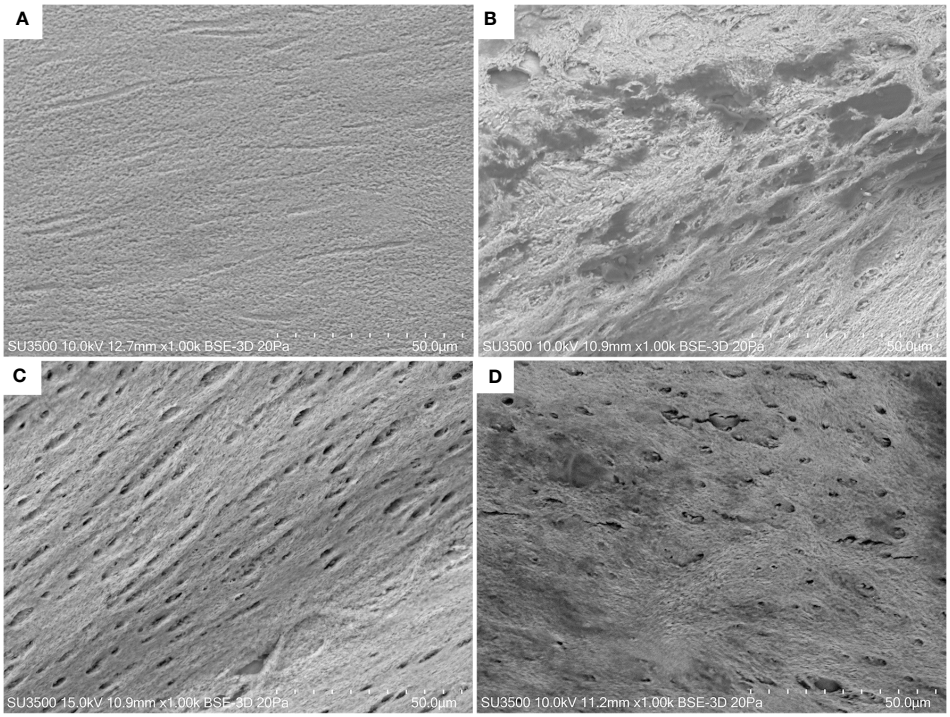

FIGURE 1
Microstructure of rainbow trout jaw. Normal fish at 1000× magnification **(A)**. Deformed fish at 1000× magnification **(A–D)**. Backscatter detector (BSD) image. Scanning Electron Microscope SU3500, Hitachi, Tokyo, Japan.

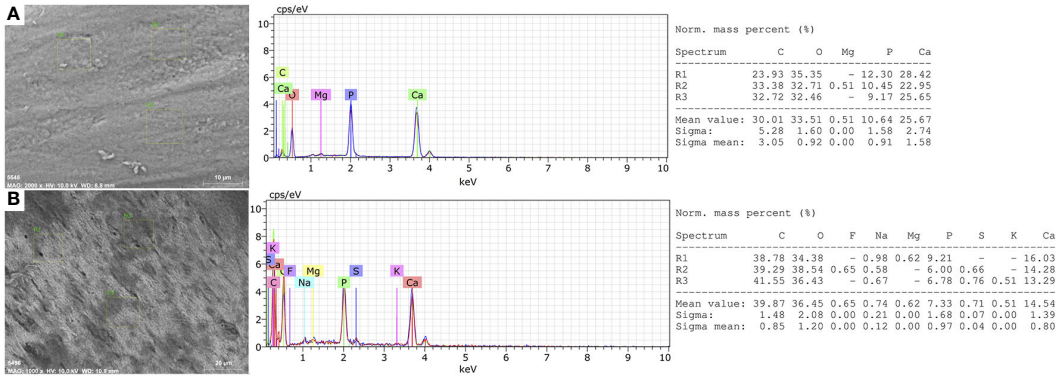

FIGURE 2
Elemental Microanalysis in the mandibular bone of rainbow trout. **(A)** Normal fish. **(B)** Deformed fish. BSD image, 1000× magnification. Scanning Electron Microscope (Hitachi SU3500, Tokyo, Japan) coupled to XFlash® Detector 410 and Quantax Esprit 1.8.1 Software controller (Bruker, Germany).

(Figure 9). The inorganic signal in the absorbed band was between 2600 and 3600 cm^{-1}, with a more pronounced peak at 3570 cm^{-1} and a weaker peak at 630 cm^{-1}. Meanwhile, the organic signals range from 2850 to 3000/1553.5/1245.9 and 1645.5 cm^{-1} for the carbonyl groups (C = O).

3.7 Bone gene expression

We divided the expression analysis into three gene groups according to their functionality: 1) transcription factors *Runx2* and *Osx* (Figure 10A), osteogenic proteins *Bmp2*, *Bmp4* (Figure 10B), and bone matrix proteins *Alp*, *Col-I*, and *Ocn* (Figure 10C), using *Ef1a* as the endogenous control. Our results showed decreased expression of *Runx2*, *Alp*, and *Ocn*, while observing increased expression of *Col-I*, *Bmp2*, and *Osx*. Bmp4 levels were reduced. The values obtained for *Shh* were undetermined and, therefore, not included in this work.

4 Discussion

Successful genetic modification initiatives have been implemented in various salmonid species to enhance the production of commercially significant characteristics (Gjedrem, 2000; Gjedrem, 2012). However, the potential adverse outcome of selective breeding has been the accumulation of inbreeding (Robertson, 1961). In fact, there is a lot of inbreeding among rainbow trout because of the selective breeding for desirable traits in small, isolated populations (D'Ambrosio et al., 2019). Prior studies have demonstrated notable negative impacts of inbreeding on the weight of female rainbow trout and the weight of their spawn (Kincaid, 1983), as well as on the number of eggs produced and the age at which spawning occurs (Su et al., 1996). In addition, Chilean studies have shown that the breeding effort has shown significant genetic improvement in body weight at harvest, with an increase of approximately 10 to 13% per generation (Neira et al., 2006; Yañez et al., 2014).

Shape differences can be found in both farmed and wild fish, but they are studied more in aquaculture because they can lower the number of fish that are produced and cause financial losses (Kause et al., 2005). Genetic diversity in populations usually goes down when culture systems are in place. This can cause inbreeding depression and other problems (Aulstad and Kittelsen, 1971). Populations with inbreeding experience slower rates of growth and reproduction as well as increased vulnerability to externally caused mortality. Inbreeding can be bad for natural populations because it lowers the genetic diversity within a population (Kause et al., 2005) and increases the number of harmful alleles that people with two copies of the recessive gene often have (Keller, 2002). Although the exact cost of inbreeding is still uncertain and subject to debate (Pusey & Wolf, 1996; Crnokrak and Roff, 1999; Frommen et al., 2008), its repercussions potentially heighten the risk of extinction (Aulstad and Kittelsen, 1971; Keller, 2002; Kerniske et al., 2021).

In Chile, the calculated genetic diversity among rainbow trout (*Oncorhynchus mykiss*) was estimated to be between 22% (Cárcamo et al., 2015) and 15.6-28.1% (Gajardo et al., 1998), which falls within the range previously reported for this species (Currens et al., 1990). Additionally, the average heterozygosity of 0.070 is higher than the value of 0.059 reported previously (Hershberger, 1992) for the same species. According to previous research on rainbow trout, the estimates show that the populations being studied have a lot of room to adapt and/or split apart. n these studies, genetic diversity, measured as heterozygosity, has been linked to key fitness characteristics (Danzmann et al., 1988).

Blood analysis was helpful in evaluating the physiological state of all species, especially fish. Testing constitutes a minimally invasive procedure and is also useful for evaluating new diets, changes in culture conditions, immune status, or stress related to fish farming management (Kaneko, 1997; Bellier, 2010; Li et al., 2010; Servicio Nacional de Pesca y Acuicultura (SERNAPESCA), 2023). The metabolic parameters obtained in this study showed differences between total protein content (53.26 g/L vs. 41.83 g/L, $p<0.01$), mainly in the globulin fraction (25.23 g/L vs. 12.69 g/L, $p<0.01$). This contrast was linked to a nutritional deficit in fish with

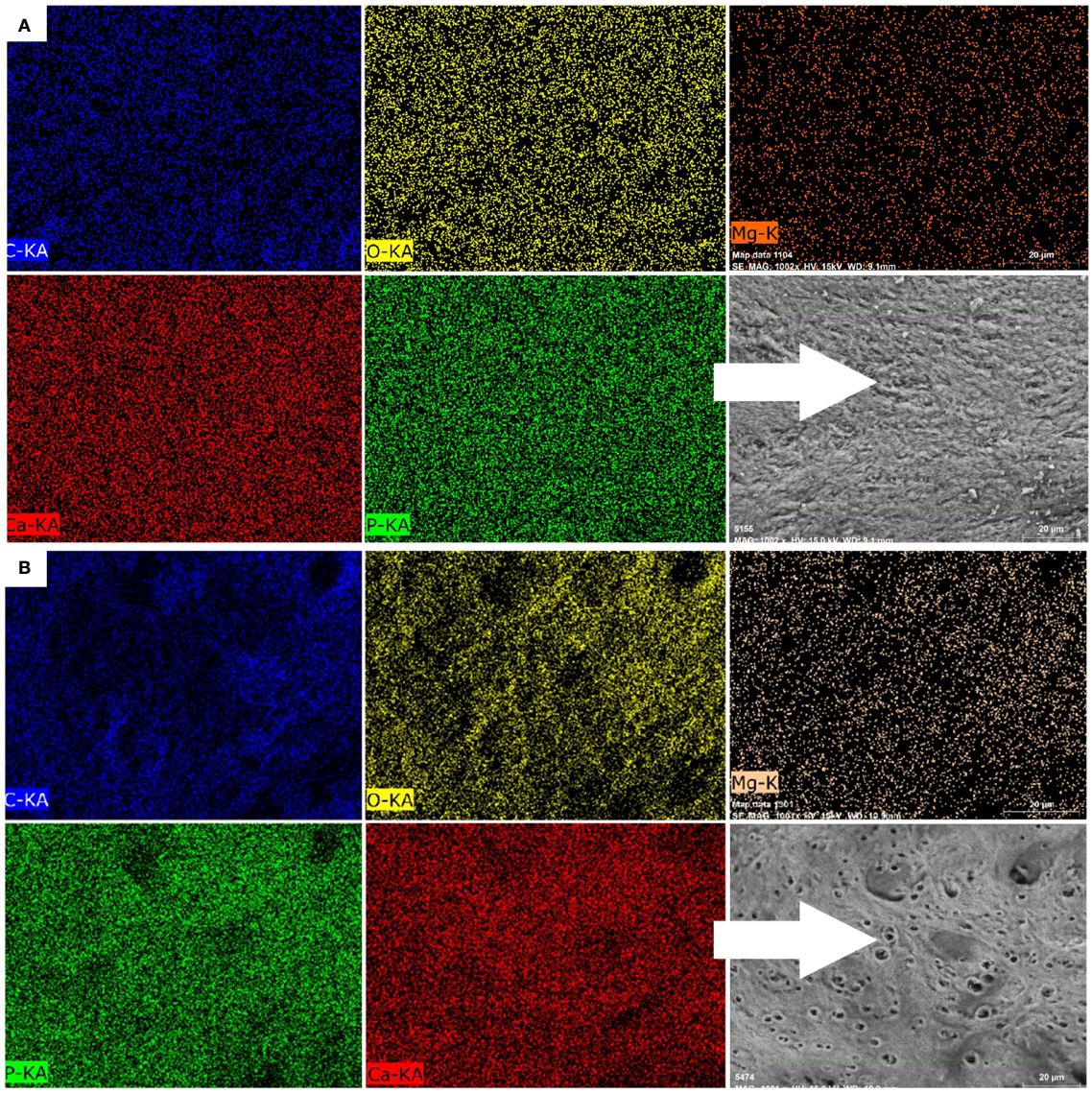

FIGURE 3
Mapping of elemental distribution in the mandibular bone of rainbow trout. **(A)** Normal fish. **(B)** Deformed fish. BSD image, 1000× magnification. Mapping of C (blue), O (yellow), Mg (orange), Ca (red), and P (green) using a scanning electron microscope (Hitachi SU3500, Tokyo, Japan) coupled to an XFlash®Detector 410 and a Quantax Esprit 1.8.1 software controller (Bruker, Germany).

mandibular deformity because they are unable to feed properly, resulting in general deterioration with decreased size and weight and a drastic loss of visceral fat.

The increased alkaline phosphatase levels reported here imply a signal of phosphorus recovery at the systemic level (10.44 mmol/L and 7.57 mmol/L, $p< 0.001$). In addition, it relates to renal reabsorption and removal by the action of enzymes (Fernández-Tresguerres et al., 2006). Calcium levels presented differences between the control (9.96 mmol/L) and the deformed fish group (9.14 mmol/L, $p<0.001$). While calcium is absorbed from the diet and through the gills, skin, and fins from the water, the soluble phosphorus forms are absorbed from the water, therefore, the most crucial pathway of phosphorus uptake comes from food, and its deficiency has been associated with demineralization and deformity (Organización de la Naciones Unidas para la Alimentación y la Agricultura (FAO), 2023; Witten et al., 2015; Rojas et al., 2016; Baejverjord et al., 2019).

The quantification of magnesium did not show significant differences between groups because, as with calcium, uptake in the gastrointestinal tract, gills, skin, and fins from the water is completed by a similar transport system (Organización de la Naciones Unidas para la Alimentación y la Agricultura, 2014). We also found decreased iron levels in deformed fish, which has been related to the development and growth problems of the fish, and microcytic anemia due to poor nutrition (4, Desjardins et al., 1987; Lall and Kaushik, 2021).

Salmonids, such as trout, can spend seasons without feeding, and their physiological state tends to be normal (Godoy et al., 2022).

10.3389/fmars.2023.1301449

TABLE 4 Semi-quantitative elemental microanalysis in mandibular bone of rainbow trout by SEM-EDX.

Mass percent (% W)	Median (minimum – maximum)		p value
	Normal Fish	Deformed Fish	
Carbon	41.09 (23.93 – 44.53)	52.31 (38.78 – 66.12)	0.003
Oxygen	28.93 (25.76 – 35.35)	27.53 (17.98 – 38.54)	0.096
Calcium	21.36 (17.69 – 28.42)	13.18 (10.26 – 16.03)	<0.001
Phosphorous	9.02 (7.53 – 12.30)	5.79 (4.15 – 9.21)	<0.001
Ca/P ratio	2.29 (1.98 – 2.68)	2.24 (1.79 – 2.81)	0.572
Magnesium	0.11 (0.00 – 0.94)	0.03 (0.00 – 0.62)	0.028
Fluoride	0.13 (0.00 – 0.86)	0.04 (0.00 – 0.65)	0.017
Sodium	0.13 (0.00 – 1.06)	0.16 (0.00 – 0.98)	0.710

However, microelement deficiency, such as calcium and phosphorus, causes skeletal alterations (Witten et al., 2015; Rojas et al., 2016; Baejverjord et al., 2019; Godoy et al., 2022). Likewise, we found higher glucose values in the mandibular deformity group (5.17 mmol/L), suggesting stress in the fish (Polakof et al., 2011; Godoy et al., 2022). The microstructural and mineralogical characterization of mandibular bone reveals a loss of mineralization that has been primarily associated with lower phosphorus levels than with any other mineral in the mandibular bone. This loss of mineralization was discrete (Figures 4, 5). The SEM-EDX analysis exhibited higher mineral values because homogenization by reduction to powder impacts the quantification in areas of interest (porosity or fractures). The porosity and surface area analysis showed a larger pore size, while the available surface area was much smaller, indicating that controls were less likely to develop microfractures (Godoy et al., 2022).

Consistent with what we obtained in TGA-DSC and mapping the elements in SEM (phosphorous was more affected than calcium), we found evidence of the inorganic forms of co-precipitation or different chemical structures, which was reflected in the XRD diffractograms and FT-IR spectra (Figures 8, 9). In the XRD analysis (Figure 8), two peaks were identified in all samples, one of greater intensity at 2θ = 32-33° and a secondary peak at 2θ = 25°. According to the analysis, they correspond to HPA and TCP, respectively. This coincides with what was reported in the literature for HPA crystal, but deformed fish showed a slightly stronger signal to 2θ = 29° which was not identified (Raina et al., 2019). We report another peak 2θ= 26-27°, which was positively identified as apatite (A), indicating tissue formation. The functional groups' analysis of FT-IR (Figure 9) compared to commercial HPA with control and deformed fish, revealed characteristic signals of structural compounds, such as hydroxyl and phosphate groups, in all samples and showed the presence of carbonate groups probably bound to HPA. We detected peaks at 2800-3000, 1553.5, and 1241.9 cm^{-1}, which correspond to the presence of N-H (amide), and another peak at 1645.5 that corresponded with carbonyl groups (C=O). Both N-H and C=O groups indicated the presence of collagen in the samples (Nesseri et al., 2020).

The gene expression analysis showed decreased *Runx2* levels in deformed fish vs. normal fish (Figure 10A), reducing *Ocn* and *Alp* expression (Figure 10C), two proteins directly related to bone mineralization. Therefore, if *Ocn* decreases, calcium fixation also decreases. Consequently, phosphorus migrates for HPA formation and deposition in the bone matrix to form new mineralized tissue. ALP data indicate a lack of signal for phosphorus resorption in bones, which explains why systemic levels increase. On the other hand, we observed increased levels of type I collagen, which could indicate bone tissue's resistance to rupture or large fractures. Instead, they progressively deform. This increase in collagen may be due to a compensatory response to preserve the structure. The increased expression of *Osx*, although it has not a relevant pathway in juvenile states, can be related to *Bmp2* induction (Figure 10B) and is independent of the expression of *Runx2* (Figure 10A) (Lee et al., 2003; Javed et al., 2008). Like increased collagen, this drastic increase in *Bmp2* levels compared to *Bmp4* can be considered an adaptive or compensatory response to interrupting the primary signal mediated by *Runx2*. Bone remodeling or repair processes are absent due to low *Bmp4* expression (Figure 10B) (Dumic-Cule et al., 2018). Likewise, studies in mice indicate that over-expression of *Bmp4* translates into less bone formation (Fernández-Sánchez and Mayani, 2008).

According to previous results in rainbow trout (Nesseri et al., 2020), the authors report a consistent Ca/P ratio due to the

TABLE 5 Superficial area and porosity analysis in rainbow trout from farmed.

Superficial Area and Porosity Analysis		
Parameters	Normal Fish	Deformed Fish
Porosity (nm)	3.49	6.41
Superficial Area (m^2/g)	76.61	52.25

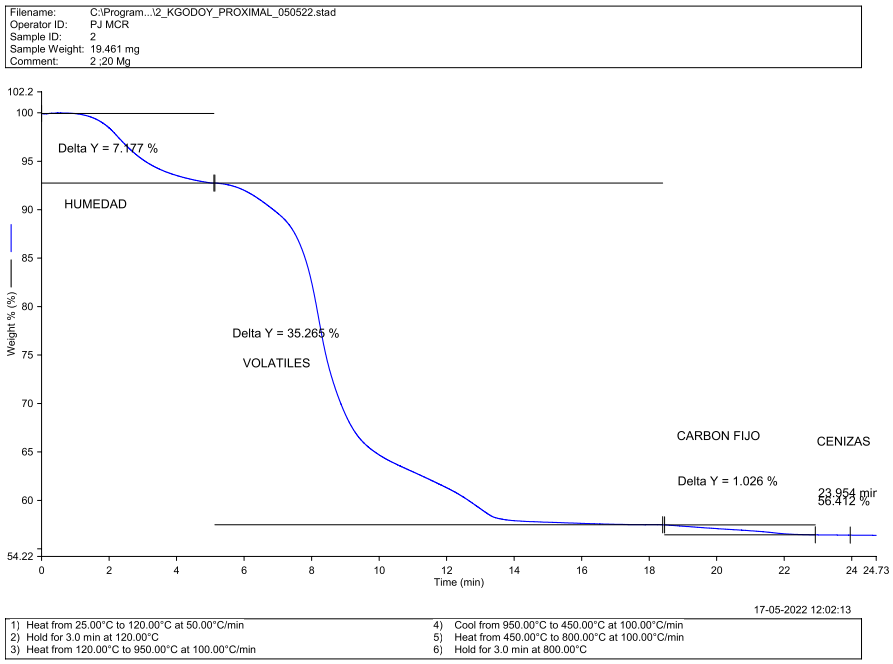

FIGURE 4
Thermogravimetric Analysis-TGA (Compositional) in mandibular bone of normal fish. TGA-DSC STA6000, Perkin Elmer, Waltham, MA, USA.

crystallographic formation of HPA and TCP (Figure 8). Given its size (nm), the porosity (indicated in Table 5) does not interfere with cell adhesion. However, it affects its biomechanical properties, as increased porosity decreases the surface area, making the bone more susceptible to microfracture. Also, deregulated *Runx2* expression, and therefore that of *Ocn* and *Col-I* (Figures 10A, C), may be directly associated with stress suffered by the fish under culture conditions. We also discovered elevated glucose levels in deformed fish, implying that this skeletal alteration can occur at any stage of development in freshwater.

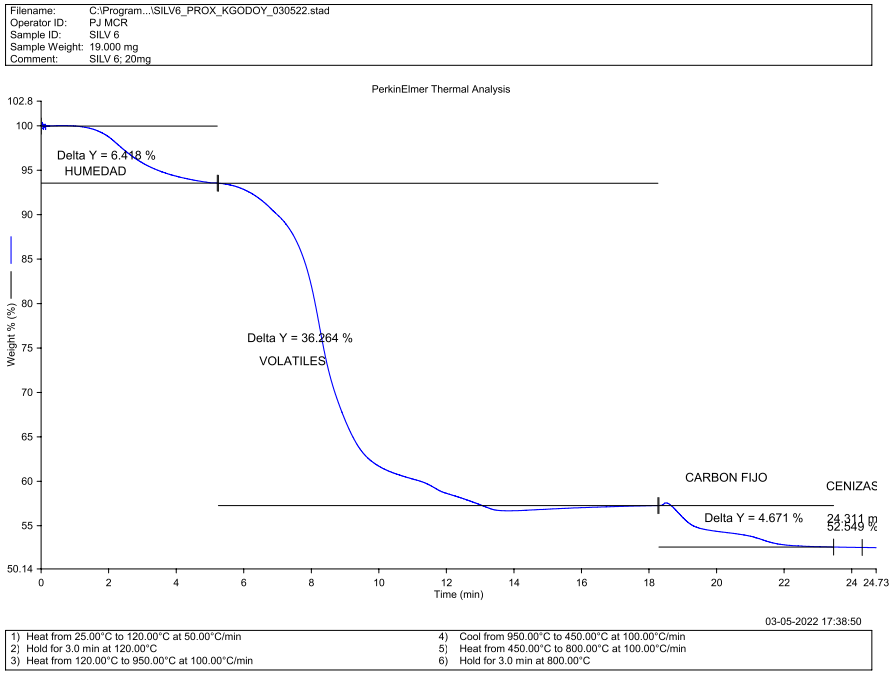

FIGURE 5
Thermogravimetric Analysis-TGA (Compositional) in mandibular bone of deformed fish. TGA-DSC STA6000, Perkin Elmer, Waltham, MA, USA.

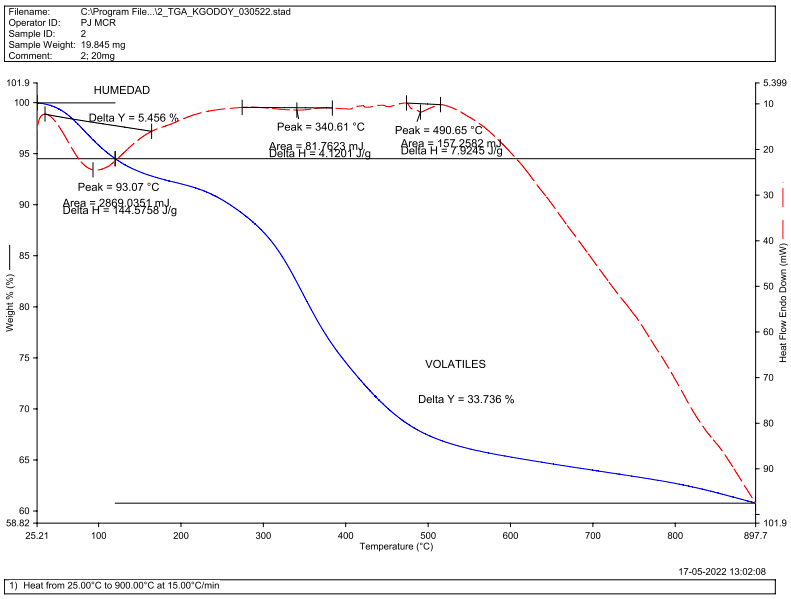

FIGURE 6
Differential Scanning Calorimetry DSC (transitions-purity) in mandibular bone of normal fish. TGA-DSC STA6000, Perkin Elmer, Waltham, MA, USA.

Regarding the mechanisms involved in decreased *Runx2* expression, the role of *Bmp2* and its influence on the induction of bone mineralization is not entirely clear. Studies indicate that even when *Bmp2* expression is high, the start of mineralization has been associated with *Smad/Runx2* interaction in the presence of Zn (Javed et al., 2008). This coupling loss may be caused by stress, resulting in decreased *Runx2* levels. Even though *Osx* expression was stimulated (Fernández-Sánchez and Mayani, 2008), it was insufficient to generate mineralization in deformed fish. In addition, endogenous BMP2 induction replaces the effect of *Runx2*, causing loss of mineralization (Kacem et al., 2000; Kacem and Meunier, 2003), increased porosity and microfractures, and advancing disease progression with deformities due to the increased type I collagen. Finally, the fish's inability to feed due to mandibular

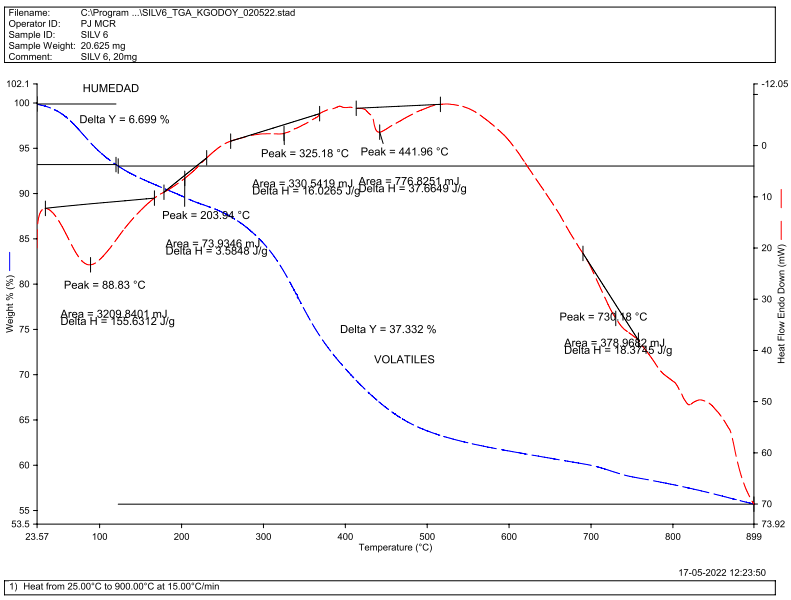

FIGURE 7
Differential Scanning Calorimetry DSC (transitions-purity) in mandibular bone of deformed fish. TGA-DSC STA6000, Perkin Elmer, Waltham, MA, USA.

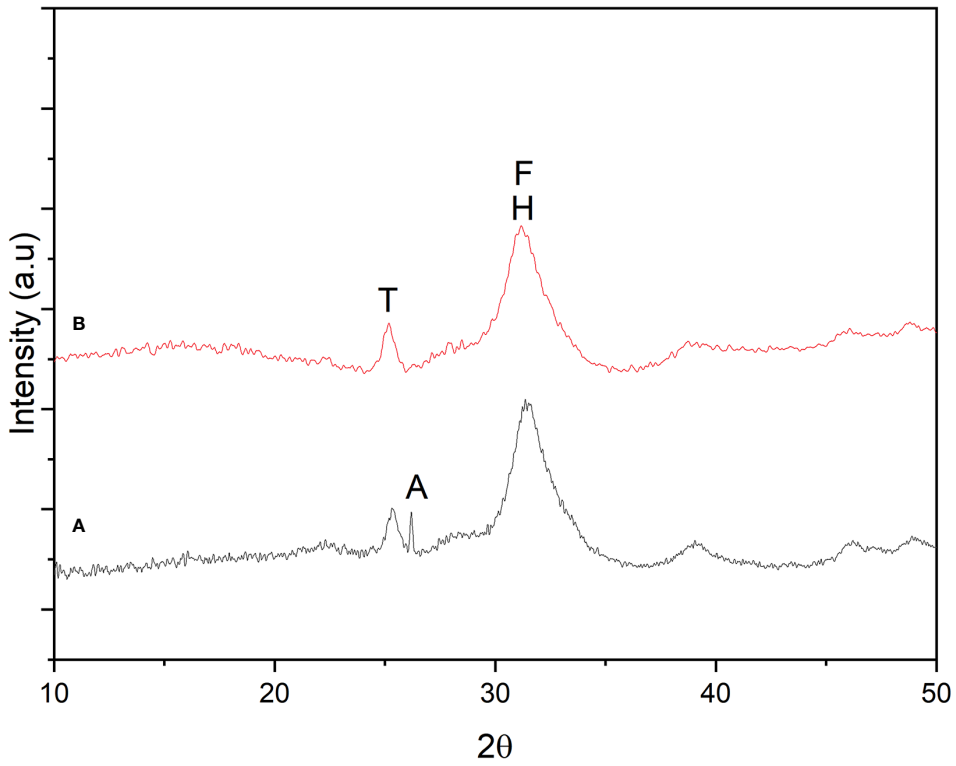

FIGURE 8
Crystallographic analysis by X-Ray Diffraction (XRD) in mandibular bone. **(A)** Normal fish. **(B)** Deformed fish. Hydroxyapatite (H), Fluorapatite (F), Tri-calcium phosphate (T), and Apatite (A) were identified using a diffractometer (2D PHAZER, Bruker, Munich, Germany).

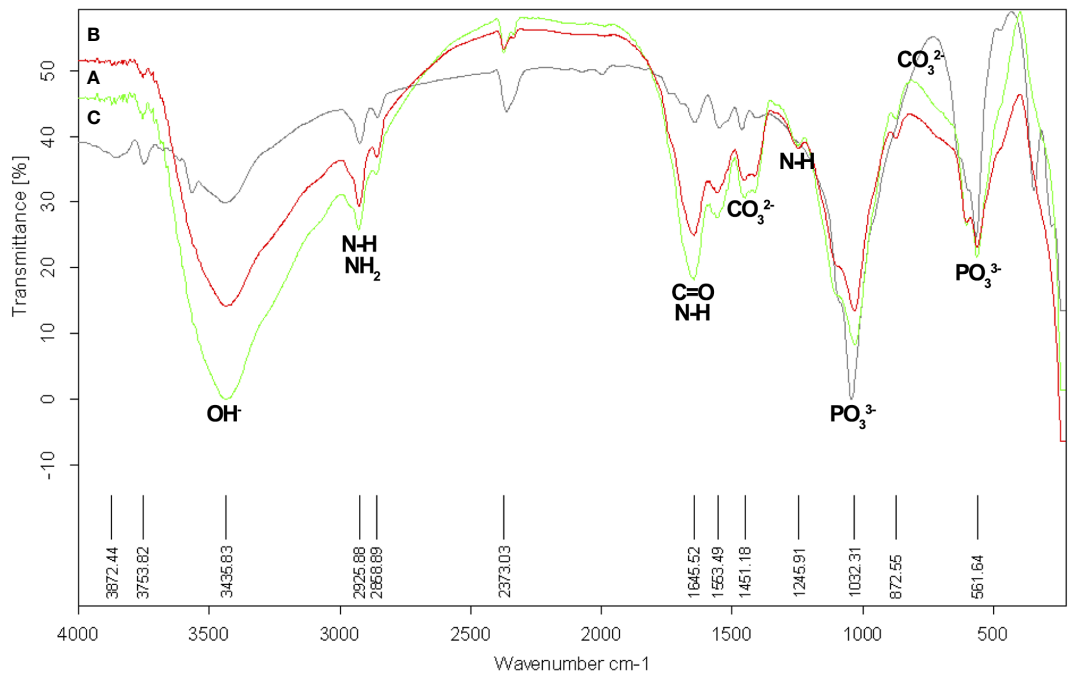

FIGURE 9
Functional groups analysis by Infrared spectroscopy (FT-IR) in mandibular bone. **(A)** Normal fish (green spectrum). **(B)** Deformed fish (red spectrum). **(C)**. Commercial HPA (black spectrum). FT-IR spectrometer TENSOR 27, Bruker, Munich, Germany.

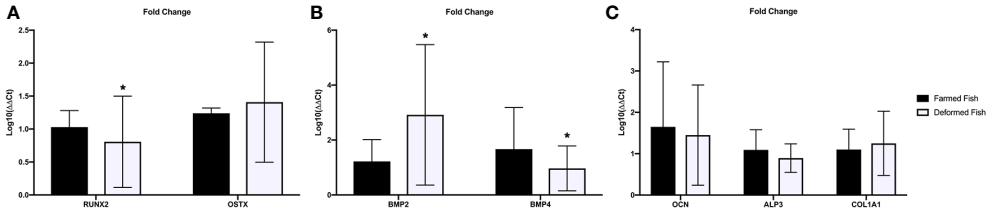

FIGURE 10
Bone gene expression. **(A)** Transcription factors, **(B)** osteogenic proteins and **(C)** bone matrix proteins mRNA Fold change was expressed as fold change using the $^{\Delta\Delta}$Ct method in deformed fish with respect to the normal fish (calibrator). Bars represent mean ± SD values of fold change per group; a: significant differences ($p<0.05$) with normal fish. *Significant differences between groups ($P<0.05$).

deformation will ultimately lead to death (Fernández-Tresguerres et al., 2006; Witten et al., 2015; Godoy et al., 2022).

5 Conclusions

The etiology of skeletal abnormalities remains an enigmatic and contentious matter in fish populations. Skeletal deformities in juvenile rainbow trout are driven by bone demineralization associated with phosphorus deficiency rather than calcium. Decreased iron and phosphorus levels are caused by poor nutrition due to an impediment to eating properly (reflected in the low content of total proteins and their fractions). This nutritional deficit does not affect calcium, as it can be absorbed through the skin and gills from the water, leaving other minerals such as magnesium unaffected. Microstructurally, demineralized bone shows microfractures and becomes more porous. Current evidence suggests it generates crystallographic formations different from HPA and TCP. Demineralization has been rather discreet or slight, which implies that there was an incomplete pathway interruption.

There was deregulation between the signals of exogenous bone tissue formation, *Bmp2*, and the expression of *Runx2*, and therefore in the expression of bone matrix proteins, such as OCN and ALP, inhibiting the formation of inorganic matrix by interfering with calcium and phosphorus fixation while also promoting an increase in the expression of organic matrix by type I collagen as a compensatory measure. Stress under culture conditions may be the most probable cause for this deregulation. It only affects a subset of the specimens in the tank and has nothing to do with developmental affections (malformations). However, genetic factors and inbreeding could also be considered as potential causes of abnormalities.

Data availability statement

The original contributions presented in the study are publicly available. This data can be found here: https://doi.org/10.6084/m9.figshare.24561739.v1.

Ethics statement

The Scientific Ethics Committee of the Universidad de La Frontera has approved the experimental protocol (N°061_20). The study was conducted in accordance with the local legislation and institutional requirements.

Author contributions

KG: Conceptualization, Formal Analysis, Investigation, Methodology, Writing - original draft, Writing - review & editing. CS: Writing - original draft, Writing - review & editing. CV: Methodology, Writing - review & editing. CM: Methodology, Writing - review & editing. BT: Methodology, Writing - review & editing. JC: Methodology, Writing - review & editing. CB: Formal analysis, Writing - review & editing. MB: Formal analysis, Writing - review & editing. SV: Formal analysis, Writing - review & editing. MR: Supervision, Writing - review & editing. LS: Conceptualization, Investigation, Supervision, Writing - review & editing.

Funding

The author(s) declare financial support was received for the research, authorship, and/or publication of this article. This research was funded by Dirección de Investigación, Universidad de La Frontera, Temuco, Chile (Grant No. DI20-TD02). Acknowledgment to Dr. Maria Eugenia Gonzalez, Director of Waste Management and Bioenergy Center (BIOREN-UFRO), who financed the use of TGA-DSC and Poroimeter analysis.

Conflict of interest

SV was employed by ADL Diagnostic Chile SpA.

The remaining authors declare that the research was conducted in the absence of any commercial or financial relationships that could be construed as a potential conflict of interest.

The author(s) declared that they were an editorial board member of Frontiers, at the time of submission. This had no impact on the peer review process and the final decision.

Publisher's note

All claims expressed in this article are solely those of the authors and do not necessarily represent those of their affiliated organizations, or those of the publisher, the editors and the reviewers. Any product that may be evaluated in this article, or claim that may be made by its manufacturer, is not guaranteed or endorsed by the publisher.

Supplementary material

The Supplementary Material for this article can be found online at: https://www.frontiersin.org/articles/10.3389/fmars.2023.1301449/full#supplementary-material

References

Aulstad, D., and Kittelsen, A. (1971). Abnormal body curvatures of rainbow trout (Salmo gairdneri) inbred fry. *J. Fish Res. Board Can.* 28 (12), 1918–1920. doi: 10.1139/f71-290

Baejverjord, G., Prabhu, P., Fjelldal, P., Albrektsen, S., Hatlen, B., Denstadli, V., et al. (2019). Mineral nutrition and bone health in salmonids. *Rev. Aquaculture* 11, 740–765. doi: 10.1111/raq.12255

Beck, G. R. J., Zerler, B., and Moran, E. (2000). Phosphate is a specific signal for induction of osteopontin gene expression. *Proc. Natl. Acad. Sci. U. S. A.* 97, 8352–8357. doi: 10.1073/pnas.140021997

Bellier, S. (2010). Interprétation etvaleur susuelles des paramètres sanguins en Biochimie clinique vétérinaire. *Rev. Francoph. Lab.* 2010, 43–56. doi: 10.1016/S1773-035X(10)70420-2

Boglione, C., Gisbert, E., Gavaia, P., Witten, P. E., Mori Moren, M., Fontagn, S., et al. (2013). Skeletal anomalies in reared European fish larvae and juveniles. Part 2: main typologies, occurrences and causative factors. *Rev. Aquac.* 5 (1), 121–167. doi: 10.1111/raq.12016

Cárcamo, C. B., Diaz, N. F., and Winkler, F. M. (2015). Genetic diversity in Chilean populations of rainbow trout, Oncorhynchus mykiss. *Lat. Am. J. Aquat. Res.* 43 (1), 59–70. doi: 10.3856/vol43-issue1-fulltext-6

Congleton, J. L., and Wagner, T. (2006). Blood-chemistry indicators of nutritional status in juvenile salmonids. *J. Fish Biol.* 69, 473–490. doi: 10.1111/j.1095-8649.2006.01114.x

Crnokrak, P., and Roff, D. A. (1999). Inbreeding depression in the wild. *Heredity.* 83, 260–270. doi: 10.1038/sj.hdy.6885530

Currens, K. P., Schreck, C. B., and Li, H. W. (1990). Allozyme and morphological divergence of rainbow trout (Oncorhynchus mykiss) above and below waterfalls in the Deschutes River, Oregon. *Copeia* 3, 730–746. doi: 10.2307/1446439

D'Ambrosio, J., Phocas, F., Haffray, P., Bestin, A., Brard-Fudulea, S., Poncet, C., et al. (2019). Genome-wide estimates of genetic diversity, inbreeding and effective size of experimental and commercial rainbow trout lines undergoing selective breeding. *Genet. Sel. Evol.* 51, 26. doi: 10.1186/s12711-019-0468-4

Danzmann, R. G., Ferguson, M. M., and Allendorf, F. W. (1988). Heterozygosity and component of fitness in a strain of rainbow trout. *Biol. J. Linn. Soc* 33, 285–304. doi: 10.1111/j.1095-8312.1988.tb00813.x

Day, T. F., Guo, X., Garrett-Beal, L., and Yang, Y. (2005). Wnt/beta-catenin signaling in mesenchymal progenitors controls osteoblast and chondrocyte differentiation during vertebrate skeletogenesis. *Dev. Cell* 8, 739–750. doi: 10.1016/j.devcel.2005.03.016

Delmas, P. D., Eastell, R., Garnero, P., Seibel, M. J., Stepan, J.Committee of Scientific Advisors of the International Osteoporosis Foundation (2000). The use of biochemical markers of bone turnover in osteoporosis. *Osteoporos. Int.* 11, 2–17. doi: 10.1007/s001980070002

Desjardins, L. M., Hicks, B. D., and Hilton, J. W. (1987). Iron catalysed oxidation of trout diets and its effect on growth and physiological response of rainbow trout. *Fish Physiol. Biochem.* 3, 173–182. doi: 10.1007/BF02180278

Downs, R. T., and Hall-Wallace, M. (2003). The American mineralogist crystal structure database. *Am. Miner.* 88, 247–250.

Ducy, P., Zhang, R., Geoffroy, V., Ridall, A. L., and Karsenty, G. (1997). Osf2/Cbfa1: a transcriptional activator of osteoblast differentiation. *Cell* 89, 747–754. doi: 10.1016/s0092-8674(00)80257-3

Dumic-Cule, I., Peric, M., Kucko, L., Grgurevic, L., Marko Pecina, M., and Slobodan Vukicevic, S. (2018). Bone morphogenetic proteins in fracture repair. *Int. Orthop.* 42, 2619–2626. doi: 10.1007/s00264-018-4153-y

Fernández-Sánchez, V., and Mayani, H. (2008). BMP4: A key regulator of embryonic development and hematopoiesis. *Rev. Inv Clin.* 60 (1), 68–74.

Fernández-Tresguerres, I., Hernández-Gil, M., Alobera, G., del Canto Pingarrón, M., and Blanco Jerez, L. (2006). Physiological bases of bone regeneration I. Histology and physiology of bone tissue. *Med. Oral. Patol. Oral. Cir. Bucal.* 11, 47–51.

Franceschi, R., and Xiao, G. (2003). Regulation of the osteoblast-specific transcription factor, Runx2: Responsiveness to multiple signal transduction pathways. *J. Cell. Biochem.* 88, 446–454. doi: 10.1002/jcb.10369

Frommen, J., Luz, C., Mazzi, D., and Bakker, T. (2008). Inbreeding depression affects fertilization success and survival but not breeding coloration in threespine sticklebacks. *Behaviour.* 145, 425–441.

Gajardo, G., Díaz, O., and Crespo, J. E. (1998). Allozymic variation and differentiation in naturalized populations of rainbow trout, Oncorhynchus mykiss (Walbaum), from southern Chile. *Aquac. Res.* 29, 785–790. doi: 10.1111/j.1365-2109.1998.tb01104.x

Gistelinck, C., Gioia, R., Gagliardi, A., and Tonelli, F. (2016). Zebrafish collagen type I: molecular and biochemical characterization of the major structural protein in bone and skin. *Sci. Rep.* 6, 21540. doi: 10.1038/srep21540

Gjedrem, T. (2000). Genetic improvement of cold-water species. *Aquac. Res.* 31, 25–33. doi: 10.1046/j.1365-2109.2000.00389.x

Gjedrem, T. (2012). Genetic improvement for the development of efficient global aquaculture: a personal opinion review. *Aquaculture* 344–349, 12–22. doi: 10.1016/j.aquaculture.2012.03.003

Godoy, K., Sandoval, C., Manterola-Barroso, C., Vásquez, C., Sepúlveda, N., Rojas, M., et al. (2022). Study of the mandibular bone microstructure and blood minerals bioavailability in rainbow trout (*Oncorhynchus mykiss*, walbaum 1792) from freshwater. *Animals* 12, 1476. doi: 10.3390/ani12121476

Gražulis, S., Chateigner, D., Downs, R. T., Yokochi, A. F. T., Quirós, M., Lutterotti, L., et al. (2009). Crystallography Open Database–An open-access collection of crystal structures. *J. Appl. Crystallogr.* 42, 726–729. doi: 10.1107/S0021889809016690

Gražulis, S., Daškevič, A., Merkys, A., Chateigner, D., Lutterotti, L., Quirós, M., et al. (2012). Crystallography Open Database (COD): An open-access collection of crystal structures and platform for world-wide collaboration. *Nucleic Acids Res.* 40, D420–D427. doi: 10.1093/nar/gkr900

Gražulis, S., Merkys, A., Vaitkus, A., and Okulič-Kazarinas, M. (2015). Computing stoichiometric molecular composition from crystal structures. *J. Appl. Crystallogr.* 48, 85–91. doi: 10.1107/S1600576714025904

Hayman, A. (2008). Tartrate-resistant acid phosphatase (TRAP) and the osteoclast/immune cell dichotomy. *Autoimmunity* 41 (3), 218–223. doi: 10.1080/08916930701694667

Hershberger, W. K. (1992). Genetic variability in rainbow trout populations. *Aquaculture.* 100, 51–71. doi: 10.1016/0044-8486(92)90339-M

Iaria, C., Spanò, N., Smeriglio, A., Capparucci, F., De Benedetto, G., Lanteri, G., et al. (2021). Massive infection of *Cystidicoloides ephemeridarum* in brown trout Salmo trutta with skeletal deformities. *Dis. Aquat. Organ.* 143, 159–168. doi: 10.3354/dao03559

Javed, A., Bae, J., Afzal, F., Gutierrez, S., Pratap, J., Zaidi, S., et al. (2008). Structural coupling of smad and runx2 for execution of the BMP2 osteogenic signal. *J. Biol. Chem.* 283 (13), 8412–8422. doi: 10.1074/jbc.M705578200

Kacem, A., Gustafsson, S., and Meunier, F. J. (2000). Demineralization of the vertebral skeleton in Atlantic salmon *Salmo salar* L. during spawning migration. *Comp. Biochem. Physiol.* 125 (4), 479–484. doi: 10.1016/s1095-6433(00)00174-4

Kacem, A., and Meunier, F. (2003). Halastatic demineralization in the vertebrae of Atlantic salmon, during their spawning migration. *J. Fish Biol.* 63, 1122–1130. doi: 10.1046/j.1095-8649.2003.00229.x

Kaneko, J. (1997). *Clinical Biochemistry of Domestic Animals* (San Diego, USA: San Diego Academic Press).

Kause, A., Ritola, O., Paananen, T., Wahlroos, H., and Mantysaari, E. A. (2005). Genetic trends in growth, sexual maturity and skeletal deformations, and rate of inbreeding in a breeding programme for rainbow trout (*Oncorhynchus mykiss*). *Aquaculture.* 247 (1–4), 177–187. doi: 10.1016/j.aquaculture.2005.02.023

Keller, L. (2002). Inbreeding effects in wild populations. *Trends Ecol. Evol.* 17 (5), 230–241. doi: 10.1016/S0169-5347(02)02489-8

Kerniske, F. F., Pena Castro, J., de la Ossa-Guerra, L. E., Mayer, B. A., Abilhoa, V., de Paiva Affonso, I., et al. (2021). Spinal malformations in a naturally isolated Neotropical fish population. *PeerJ.* 9, e12239. doi: 10.7717/peerj.12239

Kincaid, H. L. (1983). Inbreeding in fish populations used for aquaculture. *Aquaculture* 33, 215–227. doi: 10.1016/0044-8486(83)90402-7

Kirkham, G. R., and Cartmell, S. H. (2007). "Genes and Proteins Involved in the Regulation of Osteogenesis," in *Topics in Tissue Engineering*. Eds. Ashammakhi, N., Reis, R., and Chiellini, E. (Finland: University of Oulu). Available at: https://www.oulu.fi/spareparts/ebook_topics_in_t_e_vol3/

Koga, T., Matsui, Y., Asagiri, M., Kodama, T., de Crombrugghe, B., Nakashima, K., et al. (2005). NFAT and Osterix cooperatively regulate bone formation. *Nat. Med.* 11, 880–885. doi: 10.1038/nm1270

Komori, T., Yagi, H., Nomura, S., Yamaguchi, A., Sasaki, K., Deguchi, K., et al. (1997). Targeted disruption of Cbfa1 results in a complete lack of bone formation owing to maturational arrest of osteoblasts. *Cell* 89, 755–764. doi: 10.1016/s0092-8674(00)80258-5

Kowalczuk, D., and Pitucha, M. (2019). Application of FTIR method for the assessment of immobilization of active substances in the matrix of biomedical materials. *Materials* 12 (18), 2972. doi: 10.3390/ma12182972

Krossøy, C., Robin Ørnsrud, R., and Wargelius, A. (2009). Differential gene expression of bgp and mgp in trabecular and compact bone of Atlantic salmon (*Salmo salar L.)* vertebrae. *J. Anat.* 215, 663–672. doi: 10.1111/j.1469-7580.2009.01153.x

Kuo, T. R., and Chen, C. H. (2017). Bone biomarker for the clinical assessment of osteoporosis: recent developments and future perspectives. *biomark. Res.* 5, 18. doi: 10.1186/s40364-017-0097-4

Lall, S. P., and Kaushik, S. J. (2021). Nutrition and metabolism of minerals in fish. *Animals* 11, 2711. doi: 10.3390/ani11092711

Lee, M. H., Kwon, T. G., Park, H. S., Wozney, J. M., and Ryooa, H. M. (2003). BMP-2-induced Osterix expression is mediated by Dlx5 but is independent of Runx2. *Biochem. Biophys. Res. Commun.* 309, 689–694. doi: 10.1016/j.bbrc.2003.08.058

Le Luyer, J., Deschamps, M., Proulx, E., Poirier-Stewart, N., Joly-Beauparlant, C., Droit, A., et al. (2015). Establishment of a comprehensive reference transcriptome for vertebral bone tissue to study the impacts of nutritional phosphorus deficiency in rainbow trout (*Oncorhynchus mykiss*, Walbaum). *Mar. Genom.* 18, 141–144. doi: 10.1016/j.margen.2014.10.002

Li, Z. H., Velisek, J., Zlabek, V., Grabic, R., Macho, J., Kolarova, J., et al. (2010). Hepatic antioxidant status and hematological parameters in rainbow trout, *Oncorhynchus mykiss*, after chronic exposure to carbamazepine. *Chem. Biol. Interact.* 183, 98–104. doi: 10.1016/j.cbi.2009.09.009

Lin, G., and Hankenson, K. (2011). Integration of BMP, Wnt, and Notch signaling pathways in osteoblast differentiation. *J. Cell Biochem.* 112 (12), 3491–3501. doi: 10.1002/jcb.23287

Liu, Z., Shi, W., Ji, X., Sun, C., Jee, W. S., Wu, Y., et al. (2004). Molecules mimicking Smad1 interacting with Hox stimulate bone formation. *J. Biol. Chem.* 279 (12), 11313–11319. doi: 10.1074/jbc.M312731200

Liu, Y., Yao, X., Liu, Y., and Wang, Y. (2014). A fourier transform infrared spectroscopy analysis of carious dentin from transparent zone to normal zone. *Caries Res.* 48 (4), 320–329. doi: 10.1159/000356868

Lubarsky, G. V., D'Sa, R. A., Deb, S., Meenan, B. J., and Lemoine, P. (2012). The role of enamel proteins in protecting mature human enamel against acidic environments: a double layer force spectroscopy study. *Biointerphases* 7 (1), 14. doi: 10.1007/s13758-011-0014-6

Matsubara, T., Kida, K., Yamaguchi, A., Hasta, K., Ichida, F., Meguro, H., et al. (2008). BMP2 Regulates Osterix through Msx2 and Runx2 during Osteoblast Differentiation. *J. Biol. Chem.* 283 (43), 29119–29125. doi: 10.1074/jbc.M801774200

Ministerio de Economía, Fomento y Turismo, Subsecretaría de Pesca y Acuicultura and Servicio Nacional de Pesca y Acuicultura (2023b) *Resolución 1577 Exenta*. Available at: https://www.bcn.cl/leyChile/navegar?idNorma=1028550.

Ministerio de Economía, Fomento y Turismo, Subsecretaría de Pesca y Acuicultura, Servicio Nacional de Pesca y Acuicultura and Dirección Nacional (2023a) *Resolución 228 Exenta*. Available at: https://www.bcn.cl/leyChile/navegar?idNorma=1049002.

Ministerio de Economía, Fomento y Turismo, Subsecretaría de Pesca y Acuicultura, Servicio Nacional de Pesca y Acuicultura and Dirección Nacionala (2023c) *Resolución 3610 Exenta*. Available at: https://www.bcn.cl/leyChile/navegar?idNorma=1135321&idParte=0.

Nakashima, K., Zhou, X., Kunkel, G., Zhang, Z., Deng, J. M., Behringer, R. R., et al. (2002). The novel zinc finger-containing transcription factor osterix is required for osteoblast differentiation and bone formation. *Cell* 108, 17–29. doi: 10.1016/s0092-8674(01)00622-5

Neira, R., Díaz, N. F., Gall, G. A. E., Gallardo, J. A., Lhorente, J. P., and Manterola, R. (2006). Genetic improvement in coho salmon (*Oncorhynchus kisutch*). I: selection response and inbreeding depression on harvest weight. *Aquaculture* 257, 9–17. doi: 10.1016/j.aquaculture.2006.03.002

Nesseri, E., Boyatzis, S., Boukos, N., and Panagiaris, G. (2020). Optimizing the biomimetic synthesis of hydroxyapatite for the consolidation of bone using diammonium phosphate, simulated body fluid, and gelatin. *Appl. Sci.* 2, 1892. doi: 10.1007/s42452-020-03547-8

Olivares, R., and Rojas, M. (2013). Axial and appendicular skeleton of vertebrates. *Int. J. Morphol.* 31 (2), 378–387. doi: 10.4067/S0717-95022013000200003

Organización de la Naciones Unidas para la Alimentación y la Agricultura (FAO) (2023). *Manual Práctico Para el Cultivo de Trucha Arcoiris* (Santiago, Chile: Organización de la Naciones Unidas para la Alimentación y la Agricultura). Available at: https://www.fao.org/3/bc354s/bc354s.pdf.

Orilisi, G., Tosco, V., Monterubbianesi, R., Notarstefano, V., Özcan, M., Putignano, A., et al. (2021). ATR-FTIR, EDS and SEM evaluations of enamel structure after treatment with hydrogen peroxide bleaching agents loaded with nano-hydroxyapatite particles. *PeerJ* 9, e10606. doi: 10.7717/peerj.10606

Paschalis, E. P., Mendelsohn, R., and Boskey, A. L. (2011). Infrared assessment of bone quality: a review. *Clin. Orthop. Relat. Res.* 469 (8), 2170–2178. doi: 10.1007/s11999-010-1751-4

Perez-Amodio, S., Jansen, D. C., Schoenmaker, T., Vogels, I. M. C., Reinheckel, T., Hayman, A. R., et al. (2006). Calvarial osteoclasts express a higher level of tartrateresistant acid phosphatase than long bone osteoclasts and activation does not depend on cathepsin K or L activity. *Calcif. Tissue Int.* 79, 245–254. doi: 10.1007/s00223-005-0289-z

Polakof, S., Mommsen, T., and Soengas, J. (2011). Glucosensing and glucose homeostasis: From fish to mammals. *Comp. Biochem. Physiol. B.* 160, 123–149. doi: 10.1016/j.cbpb.2011.07.006

Pombinho, A. R., Laizé, V., Molha, D. M., Marques, S., and Cancela, M. L. (2004). Development of two bone-derived cell lines from the marine teleost Sparus aurata, evidence for extracellular matrix mineralization and cell-type-specific expression of matrix Gla protein and osteocalcion. *Cell Tissue Res.* 315, 393–406. doi: 10.1007/s00441-003-0830-1

Pusey, A., and Wolf, M. (1996). Inbreeding avoidance in animals. *Trends Ecol. Evol.* 11 (5), 201–206. doi: 10.1016/0169-5347(96)10028-8

Raina, D. B., Liu, Y., Isaksson, H., Tägil, M., and Lidgren, L. (2019). Synthetic hydroxyapatite: a recruiting platform for biologically active molecules. *Acta Orthop.* 91 (2), 126–132. doi: 10.1080/17453674.2019.1686865

Robertson, A. (1961). Inbreeding in artificial selection programmes. *Genet. Res.* 2, 189–194. doi: 10.1017/S0016672300000690

Rojas, M., Ramírez, E., and del Sol., M. (2016). Morphological study and mineral analysis of the lower mandible of adult atlantic salmon (*Salmo salar*) from scotland with mandibular deformation. *Int. J. Morphol.* 34 (3), 1097–1104. doi: 10.4067/S0717-95022016000300046

Saito, M., Kunisaki, N., Hirono, I., Aoki, T., Ishida, M., Urano, N., et al. (1998). Partial characterization of cDNA clones encoding the three distinct pro a chains of type I collagen from rainbow trout. *Fisheries Sci.* 64, 780–786. doi: 10.1046/j.1444-2906.2000.00052.x

Saito, M., Takenouchi, Y., Kunisaki, N., and Kimura, S. (2001). Complete primary structure of rainbow trout type I collagen consisting of 1(I)2(I)3(I) heterotrimers. *Eur. J. Biochem.* 268, 2817–2827. doi: 10.1046/j.1432-1327.2001.02160.x

Sandoval, C., Mella, L., Godoy, K., Adeli, K., and Farías, J. (2022). β-carotene increases activity of cytochrome P450 2E1 during ethanol consumption. *Antioxidants* 11 (5), 1033. doi: 10.3390/antiox11051033

Servicio Nacional de Pesca y Acuicultura (SERNAPESCA) (2023). *Clinical Pathology Manual of Salmonid Fish* (Santiago, Chile: Aquaculture Sanitary Management Program of the National Service for Fisheries and Aquaculture). Available at: http://www.sernapesca.cl/sites/default/files/part_i_introduction_version_31.01.18.pdf.

Sinha, K., and Xin Zhou, X. (2013). Genetic and molecular control of Osterix in skeletal formation. *J. Cell. Biochem.* 114 (5), 975–984. doi: 10.1002/jcb.24439

Su, G. S., Liljedahl, L. E., and Gall, G. A. E. (1996). Effects of inbreeding on growth and reproductive traits in rainbow trout (*Oncorhynchus mykiss*). *Aquaculture* 142, 139–148. doi: 10.1016/0044-8486(96)01255-0

Sugiura, S. H., McDaniel, N. K., and Ferraris, R. P. (2003). *In vivo* fractional P(i) absorption and NaPi-II mRNA expression in rainbow trout are upregulated by dietary P restriction. *Am. J. Phys. Regul. Integr. Comp. Phys.* 285, 770–781. doi: 10.1152/ajpregu.00127.2003

Theslelf, I. (1995). Homeobox genes and growth factors in regulation of craniofacial and tooth morphogenesis. *Acta Odontol. Scand.* 53 (3), 129–134. doi: 10.3109/00016359509005962

Verdelis, K., Lukashova, L., Wright, J. T., Mendelsohn, R., Peterson, M. G. E., Doty, S., et al. (2007). Maturational changes in dentin mineral properties. *Bone* 40 (5), 1399–1407. doi: 10.1016/j.bone.2006.12.061

Witten, P. E., Owen, M. A. G., Fontanillas, R., Soenens, M., McGurk, C., and Obach, A. (2015). A primary phosphorus-deficient skeletal phenotype in juvenile Atlantic salmon *Salmo salar*: the uncoupling of bone formation and mineralization. *J. Fish Biol.* 88 (2), 690–708. doi: 10.1111/jfb.12870

Yañez, J. M., Bassini, L. N., Filp, M., Lhorente, J. P., Ponzoni, R. W., and Neira, R. (2014). Inbreeding and effective population size in a coho salmon (*Oncorhynchus kisutch*) breeding nucleus in Chile. *Aquaculture* 420-421 (1), S15–S19. doi: 10.1016/j.aquaculture.2013.05.028

Zhao, B., Xing, G., and Wang, A. (2019). The BMP signaling pathway enhances the osteoblastic differentiation of bone marrow mesenchymal stem cells in rats with osteoporosis. *J. Orthop. Surg. Res.* 14, 462. doi: 10.1186/s13018-019-1512-3

Zhou, X., Zhang, Z., Feng, J. Q., Dusevich, V. M., Sinha, K., Zhang, H., et al. (2010). Multiple functions of Osterix are required for bone growth and homeostasis in postnatal mice. *Proc. Natl. Acad. Sci. U. S. A.* 107, 12919–12924. doi: 10.1073/pnas.0912855107